Spacing Statistics for Particle Impacts

Hartley H. King*
Effects Technology, Inc., Santa Barbara, Calif.

When a hypervelocity object flies through dust or rain, damage areas will occur whose centers are randomly spaced in a projection plane normal to the motion. This randomness in impact location implies that any first-principles approach to predicting damage or mass loss should be statistical. The objective of this Note is to begin such an analysis by deriving probability functions for the location and spacing of the impact centers. Specifically, we shall calculate the probability density $p_i(r_i)$ that the ith impact center, ordered by increasing distance from a given point, is located at distance r_i. This information will be required in studies which consider the mass removed in a typical impact, given that the surface already is damaged by previous impacts.

Impacts Within a Circle

Assume that the incoming particles are spaced completely at random and that many impacts have occurred in an area the size of the body. Thus, edge effects can be ignored and the statistics will be substantially independent of position. First, let us calculate for a typical impact the probability $P(K,r)$ that (in the normal projection plane) exactly K previous impact centers lie within a circle of radius r from the center of the current impact. This problem as well as its solution technique is similar to predicting the time of electron emission in vacuum tubes.[1] Since the current problem occurs in two dimensions, the derivation in Ref. 1 is modified accordingly.

Suppose that on the average there are B impact centers per unit area. It seems reasonable that the probability that a single center lies within a ring of width δr at radius r is proportional to the area of the ring, i.e.

$$P(1,\delta r) = ar\delta r \qquad \begin{array}{l} a = \text{constant} \\ \delta r \to 0 \end{array} \tag{1}$$

and the probability is negligible that more than one impact center is in δr if δr is sufficiently small

$$P(0,\delta r) + P(1,\delta r) = 1, \quad \delta r \to 0 \tag{2}$$

The probability that no impacts are in the complete circle $r+\delta r$ is found by considering the inner circle and annulus separately

$$P(0,r+\delta r) = P(0,r)P(0,\delta r) \tag{3}$$

By using this in Eqs. (1) and (2) and passing to the limit $\delta r \to 0$, we get a differential equation

$$\frac{P(0,r+\delta r) - P(0,r)}{\delta r} \approx \frac{\mathrm{d}P(0,r)}{\mathrm{d}r} = -arP(0,r) \tag{4}$$

With $P(0,0) = 1$, the solution is

$$P(0,r) = \exp(-ar^2/2) \tag{5}$$

Now consider the probability that K impacts lie in the combined circle $r+\delta r$. Proceeding in a manner similar to the foregoing,[1] we arrive at the following differential equation

$$\frac{\mathrm{d}P(K,r)}{\mathrm{d}r} = arP(K-1,r) - arP(K,r) \tag{6}$$

where $P(K,0) = 0$. The solution is a recurrence relation giving $P(K,r)$ in terms of $P(K-1,r)$

$$P(K,r) = a\exp(-ar^2/2)\int_0^r \bar{r}\exp(a\bar{r}^2/2)P(K-1,\bar{r})\mathrm{d}\bar{r} \tag{7}$$

Thus the solution of the problem posed earlier is

$$P(K,r) = \frac{(ar^2/2)^K}{K!}\exp(-ar^2/2) \tag{8}$$

which gives the probability that exactly K impact centers lie in a circle radius of r. This is a two-dimensional version of the Poisson distribution.

Now we can relate the unknown constant a to the average number of impacts per unit area B. Since $P(K,r)$ is the probability that exactly K impacts are in circle r, the average number in r is

$$\bar{K} = \sum_{K=0}^{\infty} \frac{K(ar^2/2)^K}{K!}\exp(-ar^2/2) = ar^2/2 \tag{9}$$

This result is evaluated easily by using the analogy with the Maclaurin series for xe^x. Since a circle's area is πr^2, we find for large r

$$a = 2\bar{K}_r/r^2 = 2\pi B \tag{10}$$

Thus, the probability relation Eq. (8) is obtained in terms of B, the mean number of impacts per unit area.

Distance to Neighboring Impact Centers

The mass loss from a typical impact in general depends on the previous state of surface damage. For example, mass loss will be enhanced over the virgin material loss if previous impact centers lie within about one or two characteristic damage radii. Thus, another result required in mass loss studies is the probability density $p_i(r)$ that the ith impact, ranked according to radial distance from a given point, lies within annulus δr. This is given by

$$p_i(r)\mathrm{d}r = P(1,\mathrm{d}r)P(i-1,r) \tag{11}$$

that is, one impact lies in dr and $i-1$ are in the interior circle. Thus from Eqs. (1) and (3) we get

$$p_i(r) = \frac{ar(ar^2/2)^{i-1}}{(i-1)!}\exp(-ar^2/2), \quad i>0 \tag{12}$$

The mean distance to the ith impact center and its variance are

$$\bar{r}_i = \int_0^\infty rp_i(r)\mathrm{d}r = \frac{(1.3...(2i-1))}{\sqrt{B}(i-1)!2^i} \tag{13}$$

$$\sigma_i{}^2 = \int_0^\infty (r-\bar{r}_i)^2 p_i(r)\mathrm{d}r = (i/\pi B) - \bar{r}_i^2 \tag{14}$$

Figure 1 is a plot of Eq. (12) showing the mean and standard deviation for several i. For example, the nearest center is at mean distance $\bar{r}_1 = (4B)^{-1/2}$ with variance $\sigma_1{}^2 = (4-\pi)/4\pi B$.

It should be noted that each impact is independent of other impacts. Thus, the probability with respect to angle is uniform and independent of radius. Also, joint probability densities involving several impacts will be equal to the product of the individual probability densities.

Received May 10, 1976.
Index categories: Meteoroid Protection Systems; Hypervelocity Impact; Material Ablation.

*Member of the Technical Staff. Member AIAA.

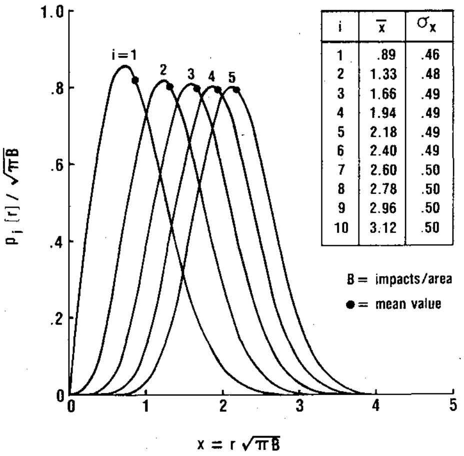

i	$\bar{x}$	σ_x
1	.89	.46
2	1.33	.48
3	1.66	.49
4	1.94	.49
5	2.18	.49
6	2.40	.49
7	2.60	.50
8	2.78	.50
9	2.96	.50
10	3.12	.50

Fig. 1 Probability density that the *i*th crater is at distance *r*.

Conclusions

Damage due to a typical impact on a surface depends on the previous state of the surface. This Note gives probability density relations for the distance to the center of the nearest damage area, the next nearest, etc. in terms of the mean number of impacts per unit area at any time. These results can be used to update probabilistic damage state specification models which involve the location of damage areas due to previous impacts.

Reference

[1] Davenport, W. B. Jr. and Root, W.L., *Random Signals and Noise*, McGraw Hill, N.Y., 1958, pp. 115-119.

Flight-Test Base Pressure Measurements in Turbulent Flow

Bruce M. Bulmer*
Sandia Laboratories, Albuquerque, N. Mex.

Nomenclature

A_B = base area
C_{Db} = base drag coefficient
Cp_b = base pressure coefficient
M = Mach number
$\dot{m}$ = total heatshield ablation (mass addition) rate
$\dot{m}/\rho_\infty V_\infty A_B$ = mass addition parameter
p = static pressure
R = base radial coordinate
R_B = base radius
R_N = nose radius
R_N/R_B = bluntness ratio
V = velocity
γ = ratio of specific heats
θ_c = cone half-angle
ρ = static density

Subscripts

b = base condition
c = local (boundary-layer edge) condition on cone immediately preceding base
∞ = freestream condition

Presented at the Open Forum Session, AIAA 11th Thermophysics Conference, San Diego, Calif., July 14-16, 1976 (no preprint). Submitted July 27, 1976; revision received Sept. 7, 1976. This work was supported jointly by the U.S. Energy Research and Development Administration and the USAF Space and Missile Systems Organization.

Index categories: Boundary Layers and Convective Heat Transfer-Turbulent; Jets, Wakes, and Viscid-Inviscid Flow Interactions; Entry Vehicle Testing.

*Member Technical Staff, Aerothermodynamics Division. Member AIAA.

Introduction

DETERMINATION of the recirculating base-flow properties in the near wake of a slender cone is important in several re-entry applications. For example, the static pressures that characterize the base-flow region are required for base drag predictions[1] and serve as a necessary boundary condition in base heating calculations.[2]

This Note presents flight-test base pressure measurements for four relatively sharp, slender re-entry vehicles (RVs). The data encompass the hypersonic, supersonic, and subsonic flow regimes ($M_\infty = 0.5$-15) and are correlated to provide an empirical prediction capability for vehicles characterized by very low heatshield ablation rates in turbulent flow (mass addition parameter $\dot{m}/\rho_\infty V_\infty A_B < 0.001$).

Base Pressure Measurements

RV Configurations

The external shapes of the four RVs were nearly identical 9° half-angle spherically blunted cones. Flights 1 and 2 were 5% blunt ($R_N/R_B = 0.05$), whereas Flights 3 and 4 were 6% blunt. Base geometry was flat for all vehicles. The ablative heatshields utilized in these tests are characterized by very low ablation rates ($\dot{m}/\rho_\infty V_\infty A_B < 0.001$) in turbulent boundary-layer flow conditions.

Instrumentation

Base pressure instrumentation incorporated two sensors for each vehicle installed at two radial positions ($R/R_B = 0.1$ and 0.8) on the base cover. Statham unbonded strain-gage type transducers were used for all tests. These were designed specifically for data acquisition in the turbulent-flow regime and were sized as either 0-68.9 or 0-103 kN/m^2 abs (0-10 or 0-15 psia) full-scale range, depending on the trajectory conditions encountered by a particular vehicle. Data were telemetered at a commutated rate of 15 samples/sec.

Each transducer was isolated from heat, vibration, and shock by mounting on a short section of soft rubber tubing, which in turn was attached to the pressure port fitting in the base cover. This provided a very short pneumatic system (tube length/port diameter ratio < 12) between the sensor and pressure port and effectively eliminated any pressure time lag.

Data Presentation

Figure 1 illustrates representative base pressure measurements as a function of flight time/decreasing altitude. Mach number regimes are identified that reveal the behavior of base pressure in various flow environments. Abrupt changes in p_b observed near $M_\infty = 4$ and $M_\infty = 1$ typify the present data. Note that this particular vehicle (Flight 2) was in subsonic flow ($M_\infty > 0.5$) during the terminal portion of re-entry.

A composite comparison of all measurements is presented in Fig. 2 in terms of the base pressure ratio and freestream Mach number (M_∞ and p_∞ were determined from postflight reconstructed trajectories that incorporated the telemetered axial accelerations and the measured ambient atmospheric conditions). These results provide a continuous variation of base pressure with Mach number throughout the range $M_\infty = 0.5$-15 and include only those data that exceed 5% of the full-scale sensor output in fully developed turbulent boundary-layer flow (established by extensive onboard thermal and dynamic motion instrumentation). Corresponding freestream Reynolds numbers (referenced to vehicle length) varied from approximately 20 million at the lowest Mach numbers to a